

Initialization effects of inter-nucleon correlations on the pion yields in heavy-ion collisions at medium energies

Zu-Xing Yang^{1,2,*}, Nicolas Michel^{1,†}, Xiao-Hua Fan³, and Wei Zuo^{1,2}

¹*Institute of Modern Physics, Chinese Academy of Sciences, Lanzhou 730000, China*

²*School of Nuclear Science and Technology, University of Chinese Academy of Sciences, Beijing 100049, China*

³*School of Physical Science and Technology, Southwest University, Chongqing 400715, China*

We study a problem of pion production in heavy ion collisions in the context of the Isospin-dependent Boltzmann-Uehling-Uhlenbeck (IBUU) transport model. In order to ponder the effect of inter-nucleon correlations on pion yields, we generated nucleon densities using two different models, the Skyrme-Hartree-Fock (SHF) model and configuration interaction shell model (SM). Indeed, inter-nucleon correlations are explicitly taken into account in SM, while they are averaged in the SHF model. As an application of our theoretical frameworks, we calculated the π^- and π^+ yields in collisions of nuclei with $A = 30 - 40$ nucleons. In order to investigate more generally the effect of shell model on the density initialization, we used different harmonic oscillator lengths b_{HO} to generate the harmonic oscillator basis. It is found that the amount of the produced π^- and π^+ mesons is larger using the SM framework with $b_{HO} = 2.5$ fm, while slight differences were found between SHF and SM results when $b_{HO} = 2$ fm. In fact, it appeared that only the use of the double π^-/π^+ ratio allows to quantitatively discriminate between the results obtained with SHF and SM model when $b_{HO} = 2$ fm.

I. INTRODUCTION

Research on heavy-ion collisions (HIC) has been extensively performed experimentally and theoretically over the past few decades [1]. While their theoretical description has relied on phenomenology for a long time [2], microscopic models have been developed in order to have a more realistic approach of HIC [1–3]. It has been shown recently that inclusion of pairing correlations can significantly modify reaction observables such as counts of emitted protons in proton-target reactions at intermediate energies by exploring the density profile of target nuclei[4]. Deformation and orientation effects have also been noticed to be important for particle production in uranium-uranium collisions at relativistic energies [5]. Consequently, both structure and reaction dynamics are important for the description of nucleus-nucleus collisions.

In order to calculate the pion yields produced during the collisions of medium and heavy nuclei, the Isospin-dependent Boltzmann-Uehling-Uhlenbeck (IBUU) transport model is often used. Recent experimental data consist of the $^{197}\text{Au} + ^{197}\text{Au}$ reaction at 400 MeV/nucleon for incident energy within the ASY-EOS experiment at the GSI laboratory [6], and of the $^{132}\text{Sn} + ^{132}\text{Sn}$ reaction at a beam energy of 0.3 GeV/nucleon, carried out at RIKEN in Japan [7]. They could provide information about the equation of state (EOS) [8–11], short-range correlations [12] and medium effects in scattering cross sections [13, 14]. Both theoretical and experimental studies have pointed out that the π meson is one of the most promising probes to study the nuclear structure and reac-

tion aspects of heavy ion collisions [9, 10, 14, 15]. The importance of π mesons for constraining the EOS of asymmetric nuclear matter was firstly pointed out by Bao-An Li et al [15]. In recent years, Stone et al have studied systematically the effects of the proton and neutron density distributions in central heavy-ion collisions, and found that the maximal neutron-to-proton ratio during the collision process is quite sensitive to the initial-state density distributions[16]. In the case of incident energy near the π meson threshold, it happens that the π meson is essentially generated by the decay of the Δ_{1232} resonant state, whereas the N^* resonant state can be ignored [1, 15]. It was also shown recently that π mesons provide a remarkably good probe to study bubble structure inside nuclei [17].

Since the original work of Skyrme in the 1950s[18] and the parameterization of the original interactions by Vautherin and Brink in the early 1970s [19], considerable efforts have been made to include effective density-dependent interactions at mean-field level to study the properties of finite nuclei and nuclear matter. In fact, the Skyrme-Hartree-Fock (SHF) model, used along with density functional theory, is one of the most efficient and widely used models to study the bulk properties of nuclei all over the nuclear chart [18, 20, 21].

As the contribution of the wave function provided by the mean-field Slater determinant describing nuclear ground states does not exceed 70%, typically, it is necessary to use models beyond mean-field to account more realistically for the effect of many-body interactions in nuclear wave functions [22]. In order to include the main effects of inter-nucleon correlations, while dealing with a numerically tractable model, we chose to use the core + valence nucleons shell model (SM) approach [22–25]. The aim of this article is then to accurately simulate experimental situations with the SHF and SM approaches, in order to identify the main effects of inter-nucleon cor-

* yangzuxing16@impcas.ac.cn

† nicolas.michel@impcas.ac.cn

relations on pion yields. Indeed, the SHF and SM approaches are typically used to theoretically calculate different types of physical observables. Bulk properties of nuclei, such as binding and Coulomb energies, mass root-mean-square (RMS) radii, neutron skins, are properly reproduced by SHF [26–28]. Using the modified Fermi distributions [29–31], radial density distributions consistent with experimental data can also be obtained [33]. Conversely, nuclear energy spectra, electromagnetic transitions, quadrupole moments and photo-nuclear reaction cross sections, i.e. observables depending on the detailed structure wave function, can be obtained with SM by using a properly devised effective interaction[22]. However, no attempt has been made to apply the density distribution of nucleons using wave functions derived from SM to initialize transport model parameters in HIC in the context of pion production. Hence, in this work, both SHF and SM approaches will be used to evaluate nucleon densities, which are then adopted in the IBUU model to calculate π^- and π^+ meson yields in HIC. We will consider nuclei of *sd*-shell, bearing $A = 30 - 40$ nucleons. Indeed, SHF can be reliably used in these nuclei due to their sizable number of nucleons, on the one hand, while SM leads to tractable shell model spaces in the considered region of nuclear chart, on the other hand. The Hamiltonians used consist of the SkM* interaction in SHF, which is widely applied for finite nuclei and nuclear matter [4, 34], while the USDB interaction will be considered as SM interaction (which one will denote as USDB-SM), as it has proved to properly describe the properties of nuclei of the *sd* shell [35]. However, as there are no experimental data available in this region of the nuclear chart, we will only compare the theoretical results obtained with SHF and SM approaches.

II. THE IBUU TRANSPORT MODEL

The phase-space distribution function $f(\vec{r}, \vec{p}, t)$ of nucleons is needed to calculate the pion yields in HIC. In the IBUU model[15] the time-evolution of $f(\vec{r}, \vec{p}, t)$ is described by the following transport equations:

$$\frac{\partial f}{\partial t} + \nabla_{\vec{p}} E \cdot \nabla_{\vec{r}} f - \nabla_{\vec{r}} E \cdot \nabla_{\vec{p}} f = I_c, \quad (1)$$

where E is the single particle energy which contains the kinetic energy E_{kin} and potential energy U , and I_c is the so-called collision item, embedding the modification of phase-space distribution function induced by elastic and inelastic two-body collisions [14]. Thus, the left and right sides of Eq.(1) represent the time evolution and collision effects involving a single particle in the nuclear mean-field, respectively.

In this model, the single nucleon potential U is a func-

tion of nucleon densities and reads [14, 36]:

$$\begin{aligned} U(\rho, \delta, \vec{p}, \tau) = & A_u(x) \frac{\rho_{\tau'}}{\rho_0} + A_l(x) \frac{\rho_{\tau}}{\rho_0} \\ & + B \left(\frac{\rho}{\rho_0} \right)^{\sigma} (1 - x\delta^2) - 8x\tau \frac{B}{\sigma + 1} \frac{\rho_0^{\sigma-1}}{\rho_0^{\sigma}} \delta \rho_{\tau'} \\ & + \frac{2C_{\tau, \tau}}{\rho_0} \int d^3 p' \frac{f_{\tau}(\vec{r}, \vec{p}')}{1 + (\vec{p} - \vec{p}')^2 / \Lambda^2} \\ & + \frac{2C_{\tau, \tau'}}{\rho_0} \int d^3 p' \frac{f_{\tau'}(\vec{r}, \vec{p}')}{1 + (\vec{p} - \vec{p}')^2 / \Lambda^2}, \end{aligned} \quad (2)$$

where $\tau, \tau' = 1/2(-1/2)$ is the isospin projection of neutrons (protons), $\delta = (\rho_n - \rho_p)/(\rho_n + \rho_p)$ denotes the isospin asymmetry, and ρ_n, ρ_p denote neutron and proton number densities, respectively. The parameters $x, A_u(x), A_l(x), B, C_{\tau, \tau}, C_{\tau, \tau'}, \sigma, \Lambda$ are standard in the IBUU model and their definition can be found in Ref.[36]. The value $x = 1$ is used for the soft symmetry energy parameter x in this work.

The following formula is used for the Δ resonance potential:

$$\begin{aligned} U^{\Delta^-} &= U_n, \quad U^{\Delta^0} = \frac{2}{3}U_n + \frac{1}{3}U_p, \\ U^{\Delta^+} &= \frac{1}{3}U_n + \frac{2}{3}U_p, \quad U^{\Delta^{++}} = U_p. \end{aligned} \quad (3)$$

The effective masses of neutron, proton and Δ resonance are directly deduced from their corresponding potential, i.e.,

$$\frac{m_B^*}{m_B} = 1 / \left(1 + \frac{m_B}{p} \frac{dU}{dp} \right). \quad (4)$$

One obtains the isospin-dependent baryon-baryon (BB) scattering cross section in medium, $\sigma_{BB}^{\text{medium}}$:

$$\begin{aligned} R_{\text{medium}}^{BB}(\rho, \delta, \vec{p}) &\equiv \sigma_{BB_{\text{elastic, inelastic}}}^{\text{medium}} / \sigma_{BB_{\text{elastic, inelastic}}}^{\text{free}}, \\ &= (\mu_{BB}^* / \mu_{BB})^2 \end{aligned} \quad (5)$$

where μ_{BB} and μ_{BB}^* are the reduced masses of the colliding baryon pairs in free space and medium, respectively, and $\sigma_{BB_{\text{elastic, inelastic}}}^{\text{free}}$ is the free BB scattering cross section. The elastic proton-proton cross section σ_{pp} and neutron-proton cross section σ_{np} are taken from experimental data, and σ_{nn} is assumed to be equal to σ_{pp} . The $N\Delta$ free elastic cross sections are assumed to be equal to nucleon-nucleon (NN) elastic cross sections at the same center of mass energy. The inelastic NN cross sections read:

$$\begin{aligned} \sigma^{pp \rightarrow n\Delta^{++}} &= \sigma^{nn \rightarrow p\Delta^-} = \sigma_{10} + \frac{1}{2}\sigma_{11} \\ \sigma^{pp \rightarrow p\Delta^+} &= \sigma^{nn \rightarrow n\Delta^0} = \frac{3}{2}\sigma_{11}, \\ \sigma^{np \rightarrow p\Delta^0} &= \sigma^{np \rightarrow n\Delta^+} = \frac{1}{2}\sigma_{11} + \frac{1}{4}\sigma_{10} \end{aligned} \quad (6)$$

and are parametrized via (see Ref.[1]):

$$\sigma_{II'}(s) = \frac{\pi(\hbar c)^2}{2p^2} \alpha \left(\frac{p_r}{p_0} \right)^\beta \frac{m_0^2 \Gamma^2 (q/q_0)^3}{(s^* - m_0^2)^2 + m_0^2 \Gamma^2}, \quad (7)$$

where:

$$\begin{aligned} s^* &= \langle M \rangle^2, \\ p_r^2(s) &= \frac{[s - (m_N - \langle M \rangle)^2][s - (m_N + \langle M \rangle)^2]}{4s}, \\ q^2(s^*) &= \frac{[s^* - (m_N - m_\pi)^2][s^* - (m_N + m_\pi)^2]}{4s^*}, \\ q_0 &= q(m_0^2), \end{aligned}$$

and I, I' represent the isospins of the initial and final states of the two nucleons, respectively. As for α, β, m_0 , and Γ , there are four parameter sets for $\sigma_{10}^d, \sigma_{11}, \sigma_{10}, \sigma_{01}$. Details concerning the value $\langle M \rangle$ and the four σ parameter sets can be found in Ref. [37].

The mass of the produced Δ baryons in Eqs.(5,6,7) is described by a modified Breit-Wigner function [38].

$$P(m_\Delta) = \frac{p_f m_\Delta \times 4m_\Delta^2 \Gamma_\Delta}{(m_\Delta^2 - m_{\Delta_0}^2)^2 + m_{\Delta_0}^2 \Gamma_\Delta^2}, \quad (8)$$

where m_{Δ_0} is the centroid of the resonance, Γ_Δ is the width of the resonance and p_f is the center of mass momentum in the $N\Delta$ channel.

As for the reaction cross section of the reverse reaction, Danielewicz and Bertsch first deduced and obtained the isospin-averaged cross section in Ref.[39]:

$$\begin{aligned} \sigma_{N\Delta \rightarrow NN} &= \left(\frac{m_\Delta p_f^2 \sigma_{NN \rightarrow N\Delta}}{2(1+\delta)p_i} \right) \\ &\times \left(\int_{m_\pi+m_N}^{\sqrt{s}-m_N} \frac{dm_\Delta}{2\pi} P(m_\Delta) \right)^{-1}, \quad (9) \end{aligned}$$

where p_f and p_i are the nucleon center of mass momenta in the NN and $N\Delta$ channels, respectively. The width of Δ resonance is given by:

$$\Gamma_\Delta = \frac{0.47q^3}{m_\pi^2 [1 + 0.6 (q/m_\pi)^2]}, \quad (10)$$

where $q = \sqrt{\left(\frac{m_\Delta^2 - m_n^2 + m_\pi^2}{2m_\Delta} \right)^2 - m_\pi^2}$, and q is the pion momentum in the Δ rest frame. For the reaction $\Delta \rightarrow \pi + N$, the classical formula $P_{\text{decay}} = 1 - \exp(-d t \Gamma_\Delta/\hbar)$ is used for the decay probability of the Δ particle. As before, a Breit-Wigner function is assumed for the $\pi + N$ cross section in the reverse reaction [38, 39]:

$$\sigma_{\pi+N} = \sigma_{\text{max}} \left(\frac{q_0}{q} \right)^2 \frac{\frac{1}{4}\Gamma_\Delta^2}{(m_\Delta - m_{\Delta_0})^2 + \frac{1}{4}\Gamma_\Delta^2}, \quad (11)$$

where q_0 is the pion momentum at the centroid of the resonance $m_{\Delta_0} = 1.232$ GeV.

The maximal cross section σ_{max} reads as follows:

$$\begin{aligned} \sigma_{\text{max}}^{\pi^+ p \rightarrow \Delta^{++}} &= \sigma_{\text{max}}^{\pi^- n \rightarrow \Delta^-} = 200 \text{mb} \\ \sigma_{\text{max}}^{\pi^- p \rightarrow \Delta^0} &= \sigma_{\text{max}}^{\pi^+ n \rightarrow \Delta^+} = 66.67 \text{mb}. \\ \sigma_{\text{max}}^{\pi^0 p \rightarrow \Delta^+} &= \sigma_{\text{max}}^{\pi^0 n \rightarrow \Delta^0} = 133.33 \text{mb} \end{aligned} \quad (12)$$

All elastic scattering and decay reactions are assumed to be isotropic in this model. Elastic scattering cross sections bear an angular distribution [40]:

$$\frac{d\sigma_{\text{el}}}{d\Omega} \propto e^{bt}, \quad (13)$$

where:

$$b = \frac{6[3.65(\sqrt{s} - 1.8766)]^6}{1 + [3.65(\sqrt{s} - 1.8766)]^6}$$

and $t = -2p^2(1 - \cos\theta)$, with p is the momentum of one particle in the center of mass frame.

Baryon-baryon collisions in the IBUU model are simulated by a Monte Carlo-based modelling process [1]. During a small time interval ($\delta t = 0.5$ fm/c), one firstly checks if two baryons are sufficiently close to interact with each other ($b_{\text{max}} = \sqrt{\sigma_{\text{nn}}^t(\sqrt{s})/\pi}$). If it is the case, one performs simulations to determine which kind of reaction should be present [1]. When a scattering reaction takes place between two nucleons, both elastic and inelastic scattering processes can arise. NN elastic reactions occur with the probability of collision $P_{\text{elastic}}(NN) = \sigma_{\text{elastic}}/\sigma_{\text{nn}}^t(\sqrt{s})$. $P_{\text{inelastic}}(NN \rightarrow N\Delta) = \sigma_{\text{inelastic}}/\sigma_{\text{nn}}^t(\sqrt{s})$ determines the probability of baryon pair formation in the $NN \rightarrow N\Delta$ reaction, with $\sigma_{\text{nn}}^t(\sqrt{s})$ the total cross section in the center-of-mass energy \sqrt{s} , and $P_{\text{elastic}}(NN) + P_{\text{inelastic}}(NN \rightarrow N\Delta) = 1$. For the baryon Δ , the same treatment has been done in our simulations, which has three branches: i. elastic scattering with the nucleon ($N\Delta$); ii. inelastic scattering with the nucleon to produce two nucleons ($N\Delta \rightarrow NN$); iii. decay to a π meson and a nucleon ($\Delta \rightarrow N\pi$). Additionally, the π mesons are absorbed by the nucleons to re-produce baryons.

The present results have been obtained using the IBUU04 program[1, 4, 8–10, 12, 14], using as inputs the nucleon densities calculated with SHF and SM, respectively. Pion yields are then determined from the Monte Carlo process described above and coded in the IBUU04 program.

III. NUCLEON DENSITIES IN THE SHF AND USDB-SM APPROACHES

The valence nucleon density distributions of the two colliding nuclei used in the IBUU model (see Eq.(2)) are isotropic. Consequently, only radial densities are

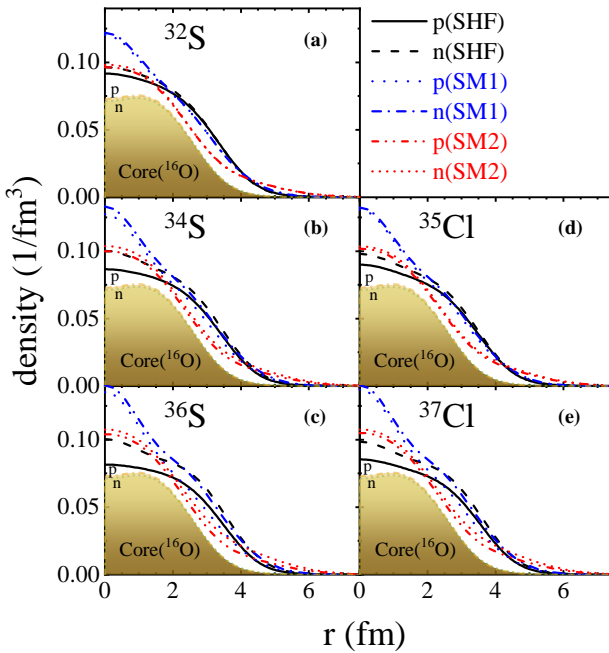


FIG. 1. (Color online) Density distributions of sulfur isotopes (a)-(c) and chlorine isotopes (d)-(e) obtained with SHF, SM1 and SM2. The normalization condition $4\pi \int_0^{r_{\max}} \rho(r)r^2 dr = A$ is used, with A the number of nucleons. The density distributions of protons and neutrons (a)-(e) of the ^{16}O core are also shown in the context of SHF, using the normalization condition $4\pi \int_0^{r_{\max}} \rho(r)r^2 dr = A_{\text{core}}$.

needed to be calculated from the SHF and USDB-SM approaches. All nucleons are active in the SHF model. Therefore, approximations are needed to evaluate a function equivalent to the USDB-SM valence nucleon density distribution in a mean-field approach. For this, one firstly calculates the total density of $^A\text{S}(A = 32, 34, 36)$, $^A\text{Cl}(A = 35, 37)$ and ^{16}O with SHF. Valence nucleon distributions in a SHF approach are then defined by subtracting of the density distribution of ^{16}O from the total density distribution of the considered nucleus:

$$\rho_r^{(n,p)}(^A\text{X(v.n.)}) = \rho_r^{(n,p)}(^A\text{X}) - \rho_r^{(n,p)}(^{16}\text{O}) \quad (14)$$

where $\text{X}=(\text{S},\text{Cl})$ and (v.n.) signifies valence nucleons.

In our SM calculations, different harmonic oscillator length $b_{HO} = 1/\alpha = \sqrt{\hbar/\mu\omega_0}$ are used. Indeed, on the one hand, in the SHF model, the length $b_{HO} = 1.42 \times A^{1/6} \approx 2.5$ fm is considered. Hence, it is for this value that the distributions issued from USDB-SM and SHF have closest maxima, so that it is physically sound to use $b_{HO} = 2.5$ fm in SM for our purpose. On the other hand, RMS nuclear charge radii play a crucial role in experimental observations. Thus, to fit the RMS of experimental nuclear charge radii in USDB-SM, we used

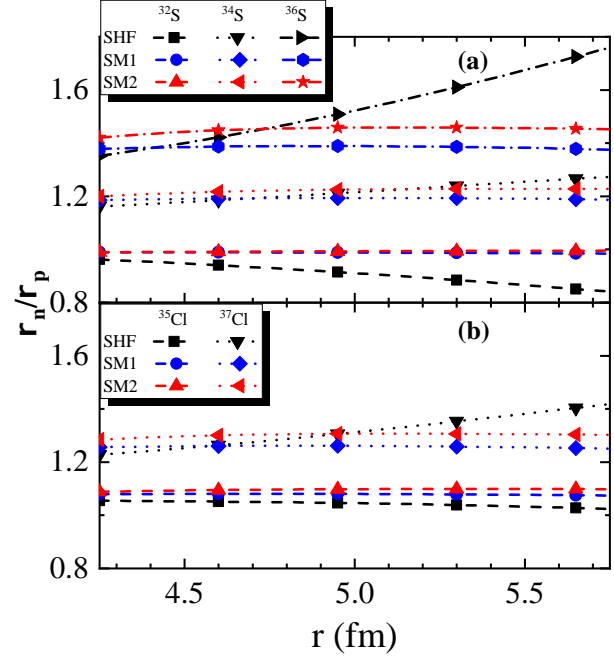


FIG. 2. (Color online) Ratio of neutron density to proton density as a function of radius in the sulfur (a) and chlorine (b), using the USDB-SM and SHF approaches.

another b_{HO} value, which is $b_{HO} = 2$ fm. For brevity, we will designate the case USDB-SM ($b_{HO} = 2$ fm) by SM1 and that of USDB-SM ($b_{HO} = 2.5$ fm) by SM2 in the following. The experimental (EXP) and calculated RMS nuclear charge radii in the different used models (SHF, SM1 and SM2) are shown in Table.I. One can see in Table.I that SM1 reproduces experimental RMS nuclear charge radii along with SHF, whereas those provided by SM2 are too large by about 0.5 fm.

TABLE I. RMS nuclear charge radii (in fm). See text for the definition of acronyms.

	SHF	SM1	SM2	EXP
^{32}S	3.256	3.282	3.804	3.261
^{34}S	3.276	3.282	3.803	3.285
^{36}S	3.300	3.282	3.803	3.298
^{35}Cl	3.328	3.310	3.857	3.365
^{37}Cl	3.348	3.310	3.856	3.384

As can be seen from Fig.1, the calculated density distributions are generated almost entirely by valence nucleons for radii larger than 4.5 fm. In the present paper, we shall consider that the reactions of interest have a large impact parameter, equal to at least 9 fm, so that one can assume that collisions will dominantly involve valence nucleons. The ^{16}O core is then not expected to play a significant role in pion production.

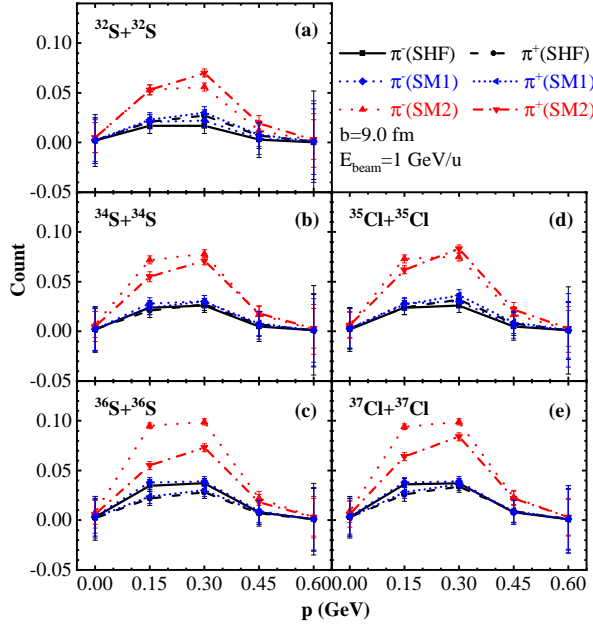


FIG. 3. (Color online) Yields of π^- and π^+ mesons as a function of momentum using different density distributions in SHF and USDB-SM in the ${}^A S + {}^A S$ and in the ${}^A Cl + {}^A Cl$ reactions. One considers sulfur isotopes with $A = 32$ (a), $A = 34$ (b) and $A = 36$ (c) nucleons in the ${}^A S + {}^A S$ reaction. For the ${}^A Cl + {}^A Cl$ reaction, one considers chlorine isotopes with $A = 35$ (e) and $A = 37$ (f). The used impact parameter and incident beam energy are 9 fm and 1 GeV/u, respectively.

We will consider the following nuclear states: ${}^{32}S(0^+)$, ${}^{34}S(0^+)$, ${}^{36}S(0^+)$, ${}^{35}Cl(3/2^+)$ and ${}^{37}Cl(3/2^+)$. The effect of nucleon-nucleon correlations is already seen in Fig.1, where the extension of SM2 density distributions is larger than those arising from SHF, while the density extension of SM1 is almost the same as that of SHF. Moreover, as can be seen in Fig.2, the ratios of neutron density to proton density in SHF and USDB-SM are close for radii around 4.5 fm. As the radius increases to about 5.5 fm, SM1 and SM2 results still remain close, while the difference between SHF and USDB-SM results increases significantly.

IV. RESULTS AND DISCUSSIONS

In order to distinguish between the different inter-nucleon correlations arising from different structural models, it is better to avoid the impact of the core and hence to consider observables depending mainly on the peripheral nature of valence nucleons distributions. π mesons are expected to be used as probes to explore peripheral properties. The inelastic processes, giving rise to

pion production, play a significant role only at beam energies close to 800 MeV/nucleon[16]. Therefore we need a higher energy to produce more mesons in order to amplify this effect in HIC. For this, we can consider a large impact parameter (9 fm, 11 fm) associated to a high incident beam energy (1 GeV/u). As already mentioned before, the most important region for this type of reaction is the tail of valence-nucleon density distributions. The different asymptotic behaviours of proton and neutron distributions may also play a significant role.

The calculated yields of π^- , π^+ are depicted on Fig.3 as a function of momentum with different initializations of valence nucleon profiles in the SHF, SM1 and SM2 for ${}^A S + {}^A S$ and ${}^A Cl + {}^A Cl$ reactions. Almost identical pion distributions are obtained with SHF and SM1, which is due to their similar nucleon density distributions. Conversely, a large difference between SHF and SM2 in π^- and π^+ yields emerges in the results, which is induced by the different nucleon density distributions arising from SM2 and SHF. The produced π meson yields are much larger with SM2 and are almost twice as large as those provided by SHF under the same entrance channel conditions. The valence nucleon density of SM2 is also more important than that of SHF when radii are larger than 4.5 fm (see Fig.1). Moreover, the yields of π^- , π^+ share a common peak at $p=0.15 - 0.30$ GeV, where the largest differences between SHF and SM2 results occur as well. For reactions involving both sulphur and chlorine isotopes, the yields of π^- mesons increase along with the number of neutrons of considered isotopes, whereas the yields of π^+ mesons are almost constant. This arises because the π^- mesons are mostly produced from neutron-neutron collisions, whereas the π^+ mesons are dominantly generated by proton-proton collisions.

Fig.4(a),(c),(e),(g),(i) show the yields of π^- , π^+ as a functions of impact parameter b with different nucleon density distribution in the SHF, SM1 and SM2 in different reactions. One can see that the pion yield decreases sharply when the impact parameter is increased to 11 fm. It is worth noting that although the pion yields generated from the SHF and SM1 models are exceptionally small and even close to zero, the pion yields of all reactions are still noticeably reduced by 25-30% compared to those obtained at a impact parameter of 9 fm. This arises because fewer nucleons are involved in the collision at larger impact parameters.

We now consider the π^-/π^+ ratio in the reactions considered above (see Fig.4(b),(d),(f),(h),(j)). The π^-/π^+ ratio increases with the mass number of the colliding nuclei in the considered reaction, because their number of protons remains the same, while their number of neutrons increases. Consequently, more π^- mesons are produced in a heavier system, so that the π^-/π^+ ratio augments. As the impact parameters change, the π^-/π^+ ratio also changes significantly. This makes it possible to distinguish between the results arising from the SHF and SM1 calculations. This is especially the case in the ${}^{32}S + {}^{32}S$ and ${}^{37}Cl + {}^{37}Cl$ reactions. Indeed, while the π^-/π^+ ratio

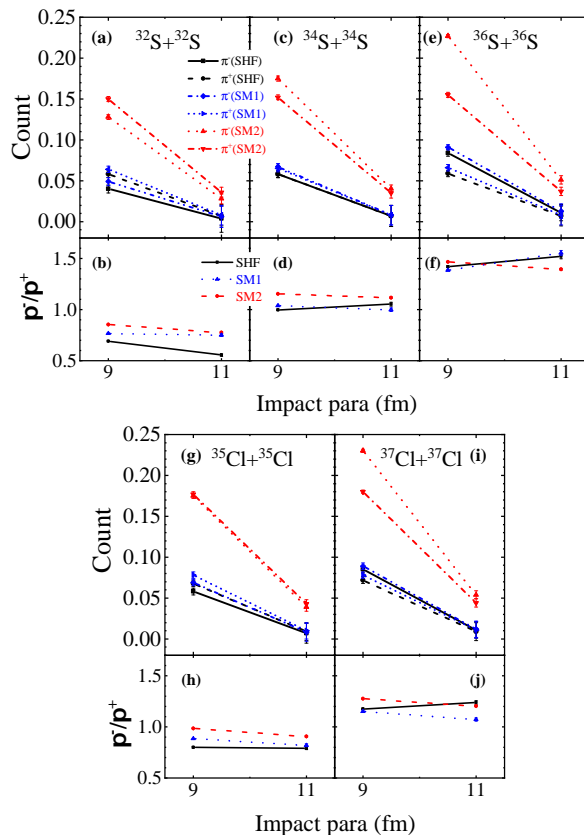


FIG. 4. (Color online) The yields of π^- , π^+ and the π^-/π^+ ratio as a function of impact parameter b with different nucleon density distribution in the SHF, SM1 and SM2 in the reactions of ${}^A\text{S} + {}^A\text{S}$ whose $A=32$ (a)-(b), $A=34$ (c)-(d), $A=36$ (e)-(f) and ${}^A\text{Cl} + {}^A\text{Cl}$ whose $A=35$ (g)-(h), $A=34$ (i)-(j) at an incident beam energy of 1 GeV/nucleon.

decreases with the increase of the impact parameter when considering the SM1 and SM2 models for both reactions, that same ratio decreases sharply in the SHF approach when considering the ${}^{32}\text{S} + {}^{32}\text{S}$ reaction, while it increases along with the impact parameter for the ${}^{37}\text{Cl} + {}^{37}\text{Cl}$ reaction. This can be related to the different density profiles obtained with the different models when radii are larger than 5.5 fm (see Fig.2). One can also use the double π^-/π^+ ratio approach [14, 41–45] in order to discriminate between the SHF and SM1 models:

$$Dr = \frac{(\pi^-/\pi^+)_{{}^{37}\text{Cl} + {}^{37}\text{Cl}}}{(\pi^-/\pi^+)_{{}^{32}\text{S} + {}^{32}\text{S}}}. \quad (15)$$

where Dr is the value of the double π^-/π^+ ratio. One

finds that $Dr(\text{SHF}) = 2.227$ and $Dr(\text{SM1}) = 1.431$, so that the double π^-/π^+ ratio varies by a factor about 1.56 in the SHF and SM1 models. This large difference indicates that the Dr is a proper observable to distinguish between SM1 and SHF. This is worth exploring from an experimental point of view.

V. SUMMARY

Pion productions in HIC depend on the nucleon density distribution of the colliding nuclei in heavy ion collisions. Nucleon densities are typically generated in a mean-field framework. However, inter-nucleon correlations may play an important role in nucleon distribution in nuclei. We have assessed the effect of valence nucleon densities of the initial colliding nuclei in SHF and USDB-SM approaches on pion yields in this work. The USDB-SM allows to include inter-nucleon correlations, which are usually neglected in theoretical calculations of pion production.

We considered colliding system of sulfur and chlorine isotopes (${}^A\text{S} + {}^A\text{S}$, ${}^A\text{Cl} + {}^A\text{Cl}$) in our applications pertaining to peripheral collisions. We noticed that pion yields are twice as large when considering inter-nucleon correlations with the harmonic oscillator length $b_{HO} = 2.5$ fm (SM2), because densities are enhanced in the surface region, and this augmentation acts similarly on π^+ and π^- meson productions. The π^-/π^+ ratio varies significantly with nucleon number. The changes in the π^-/π^+ ratio caused by the impact parameters are consistent with the variations in the density ratio of nuclei. By investigating the two reactions ${}^{37}\text{Cl} + {}^{37}\text{Cl}$ and ${}^{32}\text{S} + {}^{32}\text{S}$, which differ most significantly at 11 fm, we found that the double ratio of π^-/π^+ is a proper observable to distinguish between SM1 and SHF, for which $Dr(\text{SHF})/Dr(\text{SM1}) \simeq 1.56$ (see Eq.(15)).

Experimental pion yields analysis would provide with an interesting perspective about the study of the effect of valence nucleon densities in HIC. One could obtain information about the inter-nucleon correlations induced by the nuclear force, which is neglected when using Thomas-Fermi or SHF nucleon densities. Large differences have been noticed to occur in pion yields when nucleon densities are taken from either SHF or USDB-SM calculations. Thus, we suggest that further experimental and theoretical studies should be made to confirm or infirm the dependence of inter-nucleon correlations on the pion production process occurring in heavy ion collisions.

VI. ACKNOWLEDGEMENTS

Prof. Gao-Chan Yong is greatly thanked for his advice. This work is supported in part by the National Natural Science Foundation of China under Grant Nos. 11775275, 11435014.

[1] G. F. Bertsch, S. Das Gupta, Phys. Rep. **160**, 189(1988)

[2] R. Stock, Phys. Rep. **135**, 259(1986).

[3] H. Stocker, W. Greiner, Phys. Rep. **137**, 277(1986).

[4] X. H. Fan, G. C. Yong, W. Zuo, Phys. Rev. C **99**, 041601(R) (2019).

[5] B. A. Li, Phys. Rev. C **61**, 021903 (2000)

[6] P. Russotto *et al.*, Phys. Rev. C **94**, 034608 (2016)

[7] SYMMETRY ENERGY project, <https://groups.nscl.msu.edu/hira/sepweb/pages/home.html>

[8] Y. F. Guo, G. C. Yong, Phys. Rev. C **100**, 014617 (2019)

[9] G. C. Yong, Y. Gao, G. F. Wei, Y. F. Guo, W. Zuo, Nucl. Part. Phys. **46** 105105 (2019)

[10] S. J. Cheng, G. C. Yong, D. H. Wen, Phys. Rev. C **94**, 064621 (2016)

[11] B. A. Li, C. B. Das, S. D. Gupta, and C. Gale, Phys. Rev. C **69**, 011603(R)(2004)

[12] Z. X. Yang, X. H. Fan, G. C. Yong, W. Zuo, Phys. Rev. C **98**, 014623 (2018)

[13] J. Xu, Phys. Rev. C **84**, 064603 (2011)

[14] G. C. Yong, Phys. Rev. C **96**, 044605 (2017)

[15] B. A. Li, Phys. Rev. C **71**, 014608 (2005)

[16] J. R. Stone, P. Danielewicz, Y. Iwata, Phys. Rev. C **96**, 014612(2017)

[17] G. C. Yong, Eur. Phys. J. A, **52**, 118 (2016)

[18] T. H. R. Skyrme, Phil. Mag. **1**, 1043 (1956).

[19] D. Vautherin, D. M. Brink, Phys. Rev. C **5**, 626 (1972).

[20] M. Grasso, Prog. Part. Nucl. Phys. **106**, 256 (2019).

[21] T. H. R. Skyrme, Nucl. Phys. **9**, 615 (1959).

[22] E. Caurier, G. Martínez-Pinedo, F. Nowacki, A. Poves, A. P. Zuker, Rev. Mod. Phys. **77**, 427 (2005).

[23] Abgrall, Y. G. Baron, E. Caurier, and G. Monsonego, Phys. Lett. B **26**, 53(1967).

[24] O. Haxel, J. H. D. Jensen, H. E. Suess, Phys. Rev. **75**, 1766 (1949)

[25] M. Goppert-Mayer, Phys. Rev. **75**, 1969 (1949).

[26] T. Naito, X. Roca-Maza, G. Colò, H. Z. Liang, Phys. Rev. C **99**, 024309 (2019)

[27] Y. Zhang, Y. Chen, J. Meng, P. Ring, Phys. Rev. C **95**, 014316 (2017)

[28] C. A. Bertulani, J. Valencia, Phys. Rev. C **100**, 015802 (2019)

[29] N. Ullah, Pramana **43** No.2, 165-168(1994)

[30] D. R. Yennie, D. G. Ravenhall, R. N. Wilson, Phys. Rev. **95**, 500 (1954).

[31] M. A. Preston, Physics of the nucleus (Addison-Wesley, Reading (Mass.), 1962).

[32] H. Euteneuer, J. Friedrich and N. Voegler, Nucl. Phys. A **298**, 452 (1978).

[33] Y. Jin, X. R. Zhou, Y. Y. Cheng, H. J. Schulze, arXiv:1910.05884

[34] J. Bartel, P. Quentin, M. Brack, C. Guet, H. B. Hakansson, Nucl. Phys. A **386**, 79 (1982).

[35] B. A. Brown, W. A. Richter, Phys. Rev. C, **74**, 034315 (2006).

[36] G. C. Yong, Phys. Rev. C **93**, 044610 (2016).

[37] B. J. VerWest, R. A. Arndt, Phys. Rev. C **25**, 1979(1982)

[38] B. A. Li, A. T. Sustich, B. Zhang, C. M. Ko, Int. J. Mod. Phys. E **10**, 267 (2001).

[39] P. Danielewicz, G. F. Bertsch, Nucl. Phys. A **533**, 712(1991)

[40] J. Cugnon, T. Mizutani, J. Vandermeulen, Nucl. Phys. A **352**, 505 (1981).

[41] Sanjeev Kumar, Y. G. Ma Phys. Rev. C **86**, 051601(R) (2012)

[42] H. H. Wolter *et al.*, Prog. Part. Nucl. Phys. **62**, 402 (2009).

[43] Z. G. Xiao, B. A. Li, L. W. Chen, G. C. Yong, and M. Zhang, Phys. Rev. Lett. **102**, 062502 (2009).

[44] Z. Q. Feng and G. M. Jin, Phys. Lett. B **683**, 140 (2010).

[45] Q. Li, Z. Li, E. Zhao, and R. K. Gupta, Phys. Rev. C **71**, 054907 (2005).